EUROPEAN ORGANIZATION FOR NUCLEAR RESEARCH

CERN/EP 87-133
29 July 1987

LONGITUDINAL DISTRIBUTION OF $\pi^{\pm}$, $K^{\pm}$, PROTONS AND ANTIPROTONS PRODUCED IN 360 GeV/c π^{-}p INTERACTIONS

LEBC-EHS Collaboration

J.L. Bailly[7], C. Caso[5], E. Castelli[14], P. Checchia[8], N. Colino[6], R. Contri[5], D. Crennell[11], A. De Angelis[8], A. De Roeck[3], N. De Seriis[10], J. Duboc[9], S. Falciano[10], C. Fernandez[4], C. Fisher[11], Yu. Fisyak[12], F. Fontanelli[5], S.N. Ganguli[2], U. Gasparini[8], U. Gensch[1], S. Gentile[10], A. Gurtu[2], J.J. Hernandez[6], S.O. Holmgren[13], J. Hrubec[15], M. Iori[10], K.E. Johansson[13], M.I. Josa[6], E. Kistenev[12], H. Leutz[4], M. Mazzucato[8], L. Montanet[4], H.K. Nguyen[9], H. Nowak[4], V. Perevoztchikov[12], P. Pilette[7], A. Poppleton[4], P. Poropat[14], S. Reucroft[4], H. Rohringer[15], J.M. Salicio[6], M. Sessa[14], S. Squarcia[5], V. Stopchenko[12], U. Trevisan[5], C. Troncon[14], F. Verbeure[3], P. Vilain[3], B. Vonck[3], R. Wischnewski[1] and G. Zumerle[8]

1 Institute für Hochenergiephysik der AdW der DDR, Berlin-Zeuthen, GDR
2 Tata Institute of Fundamental Research, Bombay, India
3 IIHE ULB-VUB, Brussels, Belgium
4 CERN, European Organization for Nuclear Research, Geneva, Switzerland
5 Dipartimento di Fisica and INFN, Università di Genova, Genova, Italy
6 CIEMAT-JEN, Madrid, Spain
7 Université de l'Etat à Mons, Mons, Belgium
8 Dipartimento di Fisica, Università di Padova and INFN, Padova, Italy
9 LPNHE, Paris 6-Paris 7, Paris, France
10 Dipartimento di Fisica and INFN, Università of Roma, La Sapienza, Roma, Italy
11 Rutherford and Appleton Laboratory, Chilton, UK
12 Institute for High Energy Physics, Serpukhov, USSR
13 Institute of Physics, University of Stockholm, Sweden
14 Dipartimento di Fisica and INFN, Università Trieste, Trieste, Italy
15 Inst. für Hochenergiephysik der Osterreichischen Akademie der Wissenschaften, Vienna, Austria

Submitted to Europhysics Letters

3621P/LM/ed

ABSTRACT

Results on the longitudinal momentum distributions of $\pi^{\pm}$, $K^{\pm}$, protons and antiprotons produced in 360 GeV/c π^-p interactions are presented. They are compared with other available data and discussed in terms of π^- fragmentation.

1. INTRODUCTION

In hadronic interactions, the longitudinal distributions of the hadrons observed in the final state, with respect to the direction of the incident particles, are the ideal variables on which the fragmentation, and therefore the parton composition of the incident particles, can be tested.

We report in this letter a measurement of charged particle inclusive longitudinal differential cross sections obtained from $\pi^- p$ interactions at 360 GeV/c. The data were obtained with the European Hybrid Spectrometer (EHS) and the LExan liquid hydrogen Bubble Chamber (LEBC) exposed to a π^- beam at the CERN SPS. Details on the experimental set-up can be found elsewhere [1,2].

Since the first aim of the experiment was to study charm particles, a laser flash and the data acquisition system were triggered when an interaction had occurred with more than two charged particles detected in a set of downstream PWC's. Events with $n_{ch} = 4$, 6 and 8 were properly weighted to account for the low topology trigger inefficiency (the trigger was 100% efficient for $n_{ch} > 8$); two-prong events are removed from this analysis, due to the small trigger efficiency for this topology.

The events were reconstructed using the spectrometer information and the position of the interaction point inside the bubble chamber. We have checked on a limited sample that for particles emitted forward in the overall c.m. this technique returns identical track parameters as obtained initiating tracks in the bubble chamber and swimming them through the spectrometer.

To identify the charged particles as $\pi^{\pm}$, $K^{\pm}$, protons or antiprotons, we used the information provided by the large pictorial drift chamber ISIS. Details on ISIS and on the treatment of this information are given elsewhere [2-4]. For each interval x, x + Δx of the variable of interest (in this analysis, the relative longitudinal momentum, or Feynman-x) the proportion of $\pi^{\pm}$, $K^{\pm}$ or $p^{\pm}$ is given by a maximum likelihood function applied to the ISIS data, where the measured ionisation of the particles with momentum x, x + Δx is compared with the ionization expected for $\pi^{\pm}$,

$K^{\pm}$, p and $p^{\pm}$. This method has been shown to be bias free [3] and can be applied to the full momentum range covered by our data. However, since the statistical significance of the $K^{\pm}$ to $p^{\pm}$ separation becomes marginal above 250 GeV/c, we shall limit our investigation to $0 < x < 0.7$ for $K^{\pm}$ and $p^{\pm}$.

More than 250,000 π^- proton interactions were recorded. We shall present results based on the analysis of 175,000 interactions, for which EHS provides the most complete information.

Results on π^o and η^o production from the same experiment have been already published [5]. They will be compared to the $\pi^{\pm}$ production. To our knowledge this work represents the first attempt to measure the differential cross section for $\pi^{\pm}$, $K^{\pm}$ and $p^{\pm}$ in the π^- fragmentation region ($x > 0$) of π^-p interactions at high energy. The closest comparison which can be made is with the 58 GeV/c π^-p data of ACCMOR [6]. We have also compared our results to the K^o_s production as observed by Biswas et al. [7] in 360 GeV/c π^-p interactions. We shall compare our results to the most commonly used fragmentation models [8,9], limiting ourselves however to a semi-quantitative discussion of the main features since a more detailed comparison to the various parton models would require a better knowledge of the resonance production and, more generally, of the long and of the short-range correlations. This deeper comparison will be the subject of a forthcoming publication.

2. INCLUSIVE CROSS SECTIONS

Inclusive cross sections for $\pi^{\pm}$, $K^{\pm}$ and $p^{\pm}$, as measured for $x > 0$, are given in table 1. For completeness, we also give in table 1 the inclusive cross sections measured in the same experiment for π^o ($x > 0$), η^o($x > 0.1$) and η($x > 0.3$) [5]. The errors quoted in table 1 include an estimate of the systematic errors which may occur for $K^{\pm}$ to $p^{\pm}$ separation. As expected $\sigma(\pi^-)$ is larger than $\sigma(\pi^+)$, reflecting the nature of the incident π^-. So significant difference is observed between $\sigma(p)$ and $\sigma(\bar{p})$; also $\sigma(K^+)$ is found to be equal to $\sigma(K^-)$, indicating that most of the K^+ (and K^-) observed forward are produced in $K\bar{K}$ pairs. $\sigma(\pi^o)$ exceeds by $\sim$ 6.8 mb what one expects from isospin conservation, i.e. $\sigma(\pi^o) = 1/2\,[\sigma(\pi^+) + \sigma(\pi^-)]$. This excess may be attributed to η^o production, as we will discuss in sect. 3.1.

3. DIFFERENTIAL CROSS SECTIONS

We now present the inclusive invariant differential cross sections in terms of the relative longitudinal momentum x (Feynman variable) and of the rapidity y in the overall c.m. system:

$$x = \frac{P_\ell}{P_{max}} \qquad y = \frac{1}{2} \ell n \frac{E + P_\ell}{E - P_\ell}$$

$$F(x) = \int \frac{E^*}{P_{max}} \frac{d^2\sigma}{dx dp_T^2} dp_T^2 \qquad F(y) = \int \frac{d^2\sigma}{dy dp_T^2} dp_T^2 \ .$$

The rapidity scale expands the central region and is therefore rather suitable for a detailed study of this region.

3.1 π-meson differential cross sections

The invariant differential cross sections for π^+ and π^- are reported in figs 1(a) and 1(b) respectively. One can observe that $\frac{d\sigma}{dx}(\pi^-) > \frac{d\sigma}{dx}(\pi^+)$ over the full x-range; moreover, this difference becomes relatively larger as $x \to 1$.

The curves in both figures show the predictions of one fragmentation model (FRITIOF [10]). The DTU model [8] gives similar predictions. These models reproduce qualitatively well the general behaviour of the data, in particular the presence of a broad maximum in $\frac{d\sigma}{dy}(\pi^-)$ at $y \simeq 1$.

Fig. 1(a) contains also $d\sigma/dx\ (\pi^0)$, taken from [5]. The already mentioned isospin violation appears here very clearly and it is mostly due to a sharp peak of $d\sigma/dx\ (\pi^0)$ at $x \sim 0$; this peak is neither present in the charged particle distributions nor predicted by the fragmentation models. The change in the slope of $d\sigma/dx\ (\pi^0)$ at $x \simeq 0.15$ indicates a large contribution of π^0 from resonance decay; furthermore, the regularity of the $\pi^\pm$ spectra in the same x-region implies that the contributing resonances must have a relatively large asymmetry in charged and neutral pion production. This fact confirms the presence of a decay like $\eta^0 \to 3\pi^0$, $\pi^+\pi^-\pi^0$; a large fraction of these η^0 may come from η' decay. An abundant central production of π^0 and η^0 has already been observed at the SPS collider [11] and was interpreted in terms of gluon-gluon interactions [12]. To explain the excess of π^0 as observed in the present experiment, one needs to introduce a central η, η' production cross section of the

order of ~ 10 mb; this value is not in disagreement with the results obtained from a smooth extrapolation of the values of table 1.

3.2 K-meson differential cross sections

Figs 2(a) and 2(b) show the invariant $K^{\pm}$ differential cross sections as a function of x and y, respectively. The curves correspond to the fragmentation model predictions and indicate a fair agreement (within 20%) with the experimental measurements. The 58 GeV/c ACCMOR results [6] for $\pi^- \to K^{\pm}$ at $x > 0.6$ are also shown in fig. 2(a); in the small overlapping region of the two experiments, $0.6 < x < 0.7$, we find an excellent agreement. For sake of completeness, we also exhibit in fig. 2(b) the rapidity distribution of K^o_s taken from ref. [7].

In the central region, our data show that the K^+ cross section is ~ 1.5 times larger than the K^- cross section. Moreover, the K^+ spectrum is peaked around $x \simeq 0$, indicating a large contribution of indirect K^+ from resonance decay, mostly K^*. If these K^* are the fragments of the incident π^-, K^{*-} and K^{*o} should dominate over K^{*+} and $\bar{K}^{*o}$, leading to the relation:

$$\sigma(K^+) \sim 2\sigma(K^-).$$

If we assume a total suppression of direct K^+ and K^{*+} production, one may try to estimate the direct K^- production, given by:

$$\frac{d\sigma}{dx}(K^-_{dir}) = \frac{d\sigma}{dx}(K^-) - \frac{1}{2}\frac{d\sigma}{dx}(K^+).$$

This difference is shown in fig. 2(a). It is characterized by a broad maximum centred at $x \sim 0.2$.

3.3 Proton and antiproton differential cross sections

The invariant p and $\bar{p}$ differential cross sections are displayed in figs 3(a) and 3(b) for x and y respectively.

Above $x \simeq 0.05$, $d\sigma/dx\,(p) \simeq d\sigma/dx\,(\bar{p})$, as expected, in first approximation, for $\pi \to p(\bar{p})$.

Below $x \simeq 0.05$, $d\sigma/dx\,(p)$ rises rapidly, whereas $d\sigma/dx\,(\bar{p})$ flattens. The rapid rise of $d\sigma/dx\,(p)$ reflects the tail of the target proton fragmentation.

The close resemblance of the proton and antiproton spectra for $x > 0.1$ suggests a common production mechanism. Both p and $\bar{p}$ have a single quark in common with the incident π^-. In the colour string phenomenology approach, equal cross section means equal probability to find (uu) and (ud) diquarks in the pion sea. Extending this approach to strange particles, one would expect equal production of Λ and $\bar{\Lambda}$ at $x > 0.1$ and $d\sigma/dx$ (Λ, $\bar{\Lambda}$) should be related to $d\sigma/dx$ (p, $\bar{p}$) by the strange quark suppression factor $\lambda_s = 0.27$. We show in fig. 3(b) $d\sigma/dy$ (Λ) and $d\sigma/dy$ ($\bar{\Lambda}$) obtained by Biswas et al. [7], multiplied by $1/\lambda_s = 3.7$. The agreement with $d\sigma/dy$ (p, $\bar{p}$) in the forward hemisphere ($y > 0$) is fairly good.

The curves drawn on figs 3(a) and 3(b) correspond to the fragmentation model predictions.

As for the $K^{\pm}$ distributions, the strange quark and diquark suppression factors, two sensitive parameters of these models, were not adjusted to our data but taken from the adjustments made on $e^+e^- \rightarrow$ hadrons at $\sqrt{s} = 29$ GeV ($\sqrt{s} = 26$ GeV in the present experiment).

Whereas in the $K^{\pm}$ case the values predicted for cross sections were in fair agreement with the observation, indicating that $\lambda_s = 0.27$ is equally good for $e^+e^- \rightarrow$ hadrons and $\pi^- \rightarrow$ hadrons, one finds a striking disagreement in the $p^{\pm}$ indicating that baryons and antibaryons are produced two times more copiously in $e^+e^- \rightarrow$ hadrons than in π^- fragmentation, at comparable c.m. energies. This difference between $e^+e^- \rightarrow$ hadrons and π^- fragmentation may suggest that the comparison should not be made at the same total c.m. energy, or that gluon jets, which are present in e^+e^- data and not in π^- fragmentation, have a richer p, $\bar{p}$ component than quark hadronisation chains.

The results presented in this letter are in good agreement with the global picture expected for π^- fragmentation by the two hadronisation chain of the DTU model [8] as well as FRITIOF [10]. They however suggest that some additional η, η' production mechanism is at work in the central region.

REFERENCES

[1] M. Aguilar-Benitez et al., Nucl. Instr. Meth. 205 (1983) 79.

[2] M. Aguilar-Benitez et al., Z. Phys. C31 (1986) 491.

[3] W.W.W. Allison et al., Nucl. Instr. Meth. 224 (1984) 396.

[4] Yu. Fisjak et al., Minimum bias events from EHS, CERN-EP-EHS-LEDA 87-15.

[5] M. Aguilar-Benitez et al., Z. Phys. C34 (1987) 419.

[6] F. Pauss et al., Z. Phys. C27 (1985) 211.

[7] N.N. Biswas et al., Nucl. Phys. B167 (1980) 41.

[8] A. Capella, U. Sukhatme and J. Tran Thanh Van, Z. Phys. C3 (1980) 329.

[9] B. Andersson, G. Gustafson, G. Ingelman and T. Sjostrand, Phys. Rep. 97 (1983) 33.

[10] B. Andersson, Lund preprint LUTP 86-3.

[11] C. Conta, Third Topical Workshop on proton-antiproton physics, Geneva (1983) 50.

[12] S.P. Baranow and A.A. Komar, Letter to JETF 42 (1985) 467.

TABLE 1

Inclusive production cross sections for different particles. The first errors are statistical. The second ones are systematics, to take into account uncertainties in particle identification. Two-prong events have been removed from the analysis.

	x range	σ(mb)
π^+	0 - 1.0	37.80 ± 0.17 ± 0.13
π^-	0 - 1.0	49.10 ± 0.23 ± 0.14
π^o	0 - 1.0	49.7 ± 1.0 ± 1.1
K^+	0 - 1.0	2.95 ± 0.08 ± 0.10
K^-	0 - 1.0	2.80 ± 0.11 ± 0.04
p	0 - 1.0	1.01 ± 0.03 ± 0.02
$\bar{p}$	0 - 1.0	1.08 ± 0.04 ± 0.02
η	0.1 - 1.0	3.1 ± 0.5
η'	0.3 - 1.0	2.9 ± 1.4

FIGURE CAPTIONS

Fig. 1 π^+ and π^- invariant differential cross sections as a function of: (a) Feynman-x; (b) rapidity. The π^o data reported in 1(a) are taken from ref. [5]. The curves in both figures represent the FRITIOF [10] predictions for the corresponding particles.

Fig. 2 K^+ and K^- invariant differential cross sections as a function of: (a) Feynman-x; (b) rapidity. The curves are the FRITIOF [10] predictions. The K^o data shown in 2(b) are from ref. [7]. Direct K^- are defined in the text.

Fig. 3 Proton and antiproton differential cross sections as a function of: (a) Feynman-x; (b) rapidity. The curves are the FRITIOF [10] predictions. The Λ and $\bar{\Lambda}$ data are taken from ref. [7].

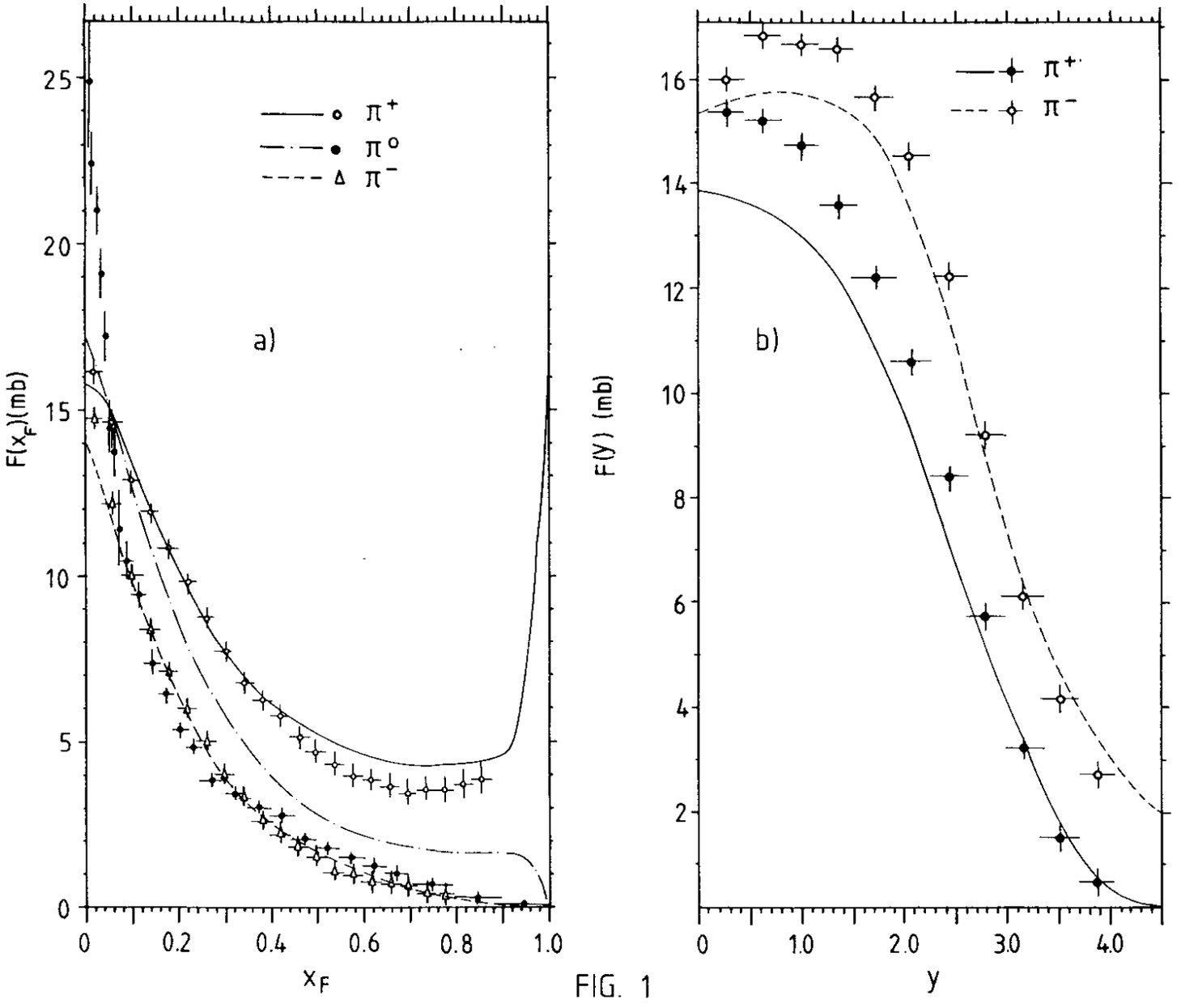
a)
b)
π^+
π^0
π^-
$F(x_F)$(mb)
x_F
F(y) (mb)
y
0
0.2
0.4
0.6
0.8
1.0
1.0
2.0
3.0
4.0
2
4
5
6
8
10
12
14
15
16
20
25

FIG. 1

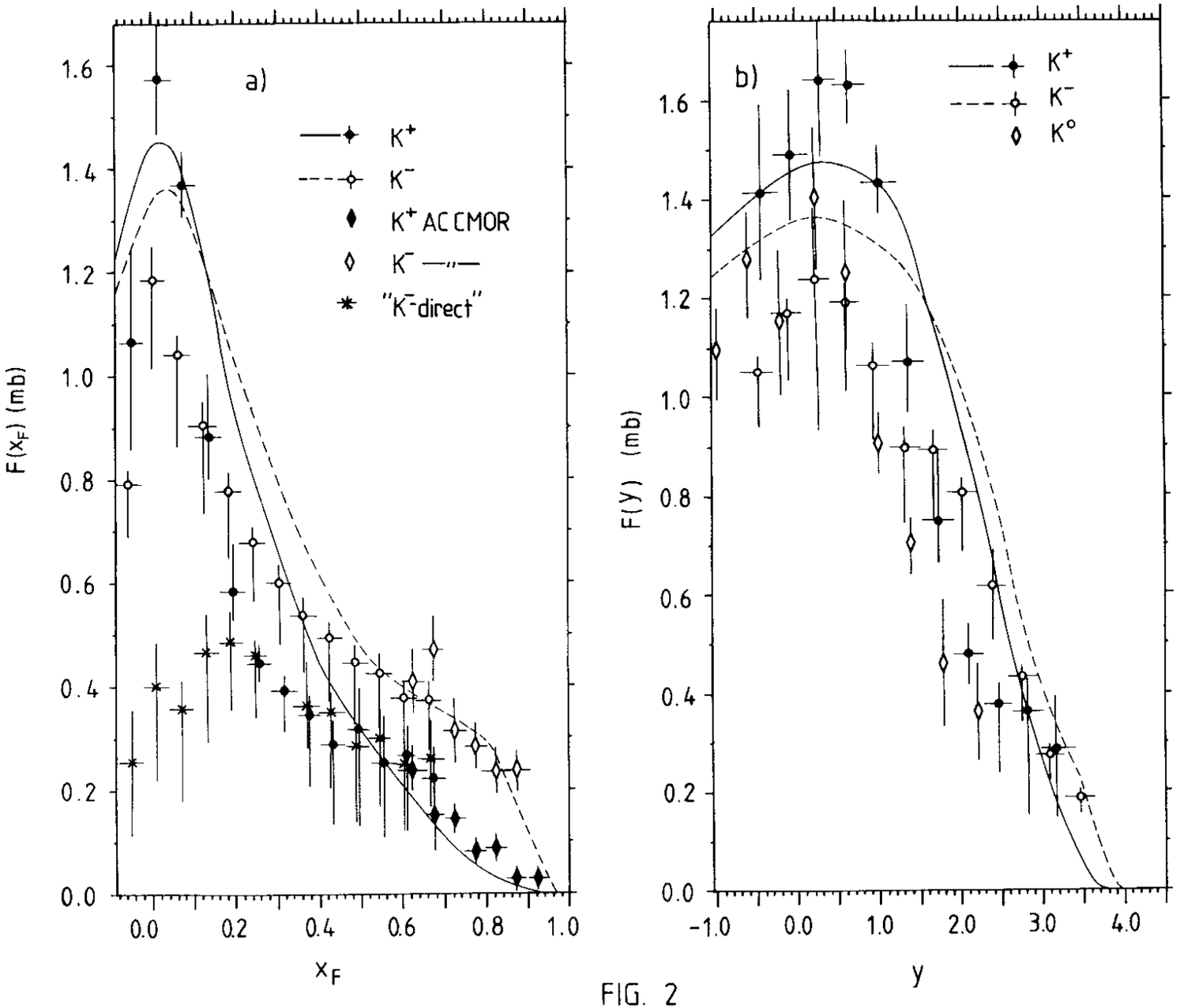
a)
b)
K+
K−
K+ ACCMOR
K− —"—
"K−direct"
K°
F(xF) (mb)
F(y) (mb)
xF
y
0.0
0.2
0.4
0.6
0.8
1.0
1.2
1.4
1.6
-1.0
1.0
2.0
3.0
4.0

FIG. 2

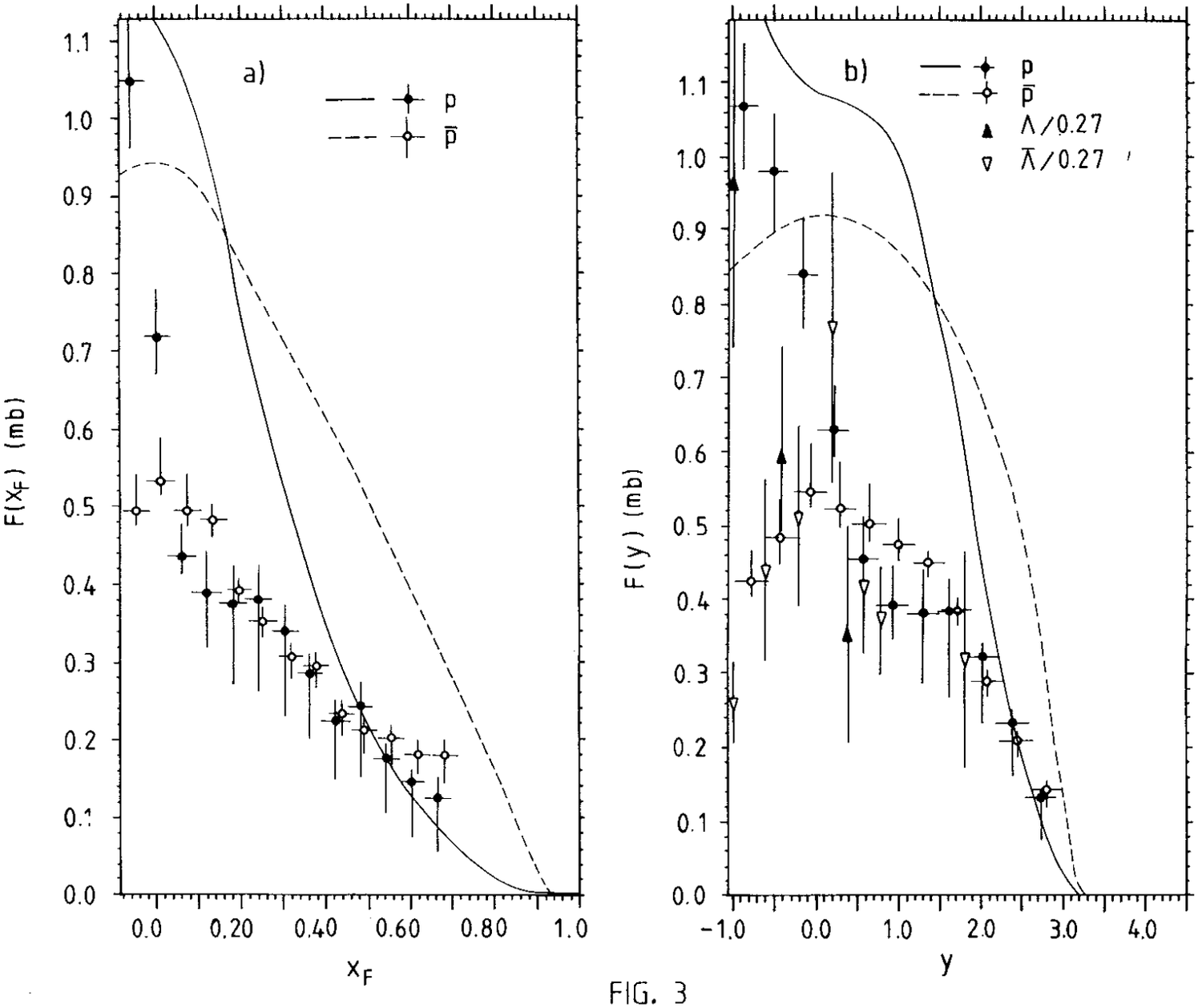
a)
p
$\bar{p}$
$F(x_F)$ (mb)
x_F
0.0
0.20
0.40
0.60
0.80
1.0
b)
p
$\bar{p}$
Λ/0.27
$\bar{\Lambda}$/0.27
F(y) (mb)
y
-1.0
0.0
1.0
2.0
3.0
4.0

FIG. 3